AIP | Review of Scientific Instruments

Top-up operation at Pohang Light Source-II

I. Hwang, J. Y. Huang, M. Kim, B.-J. Lee, C. Kim, J.-Y. Choi, M.-H. Kim, H. S. Lee, D. Moon, E. H. Lee, D.-E. Kim, S. H. Nam, S. Shin, and Moohyun Cho

Citation: Review of Scientific Instruments **85**, 055113 (2014); doi: 10.1063/1.4878256
View online: http://dx.doi.org/10.1063/1.4878256
View Table of Contents: http://scitation.aip.org/content/aip/journal/rsi/85/5?ver=pdfcov
Published by the AIP Publishing

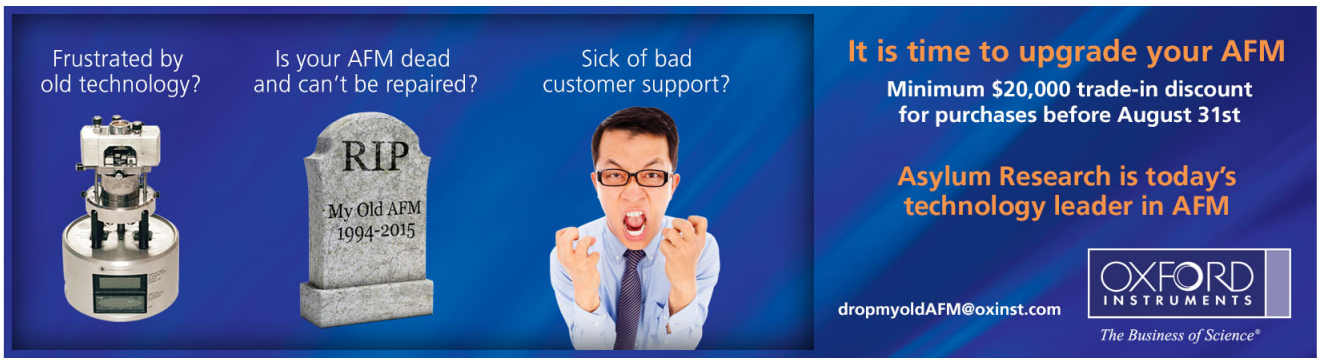

Top-up operation at Pohang Light Source-II

I. Hwang,[1] J. Y. Huang,[1] M. Kim,[1] B.-J. Lee,[1] C. Kim,[1] J.-Y. Choi,[1] M.-H. Kim,[1] H. S. Lee,[1] D. Moon,[1] E. H. Lee,[1] D.-E. Kim,[1] S. H. Nam,[1] S. Shin,[1] and Moohyun Cho[2]
[1]*Pohang Accelerator Laboratory, Pohang, Kyungbuk 790-834, South Korea*
[2]*Department of Physics, POSTECH, Pohang, Kyungbuk 790-834, South Korea*

(Received 28 August 2013; accepted 5 May 2014; published online 23 May 2014)

After three years of upgrading work, PLS-II (S. Shin, Commissioning of the PLS-II, JINST, January 2013) is now successfully operating. The top-up operation of the 3 GeV linear accelerator had to be delayed because of some challenges encountered, and PLS-II was run in decay mode at the beginning in March 2012. The main difficulties encountered in the top-up operation of PLS-II are different levels between the linear accelerator and the storage ring, the 14 narrow gap in-vacuum undulators in operation, and the full energy injection by 3 GeV linear accelerator. Large vertical emittance and energy jitter of the linac were the major obstacles that called for careful control of injected beam to reduce beam loss in the storage ring during injection. The following measures were taken to resolve these problems: (1) The high resolution Libera BPM (see http://www.i-tech.si) was implemented to measure the beam trajectory and energy. (2) Three slit systems were installed to filter the beam edge. (3) De-Qing circuit was applied to the modulator system to improve the energy stability of injected beam. As a result, the radiation by beam loss during injection is reduced drastically, and the top-up mode has been successfully operating since 19th March 2013. In this paper, we describe the experimental results of the PLS-II top-up operation and the improvement plan. © *2014 AIP Publishing LLC*. [http://dx.doi.org/10.1063/1.4878256]

I. INTRODUCTION

In order to stabilize the stored electron beam orbit as well as the synchrotron radiation flux, a small amount of beam current had to be injected into the stored beam to keep its current almost constant during top-up operation.[1] PLS-II[2] had originally planned to start top-up injection from March 2012. Unfortunately, however, it had to be delayed because of a large beam loss during beam injection. After improving on the beam injection for a year in 2012, PLS-II has been successfully performing the top-up operation since March 2013.

In general, a small vertical aperture like the in-vacuum undulator invokes the need for careful control of injected beam to prevent beam loss during the top-up injection. Figure 1 shows the nominal ID gap changes during user run of PLS-II. A total of ten in-vacuum undulators have been in operation and four more are scheduled to be installed later. The minimum full gap for the in-vacuum undulator operation is 6 mm (operation gap of in-vacuum undulators can be reduced more than 6 mm by user request). Figure 2 shows the radiation dose in the beam line during the top-up test in May 2012. Most beam line radiation detectors exceeded the allowable radiation dose (3 μSv/h). It was clear that the main cause of excessive radiation dose was the beam loss through the small physical aperture in the in-vacuum undulator, since the radiation dose was alleviated to allowable dose level in the case of the open gap of the in-vacuum undulator as shown in Fig. 2. However, we had to drastically improve the radiation dose to ensure radiation safety during the top-up operation.

The challenges of operating the new PLS-II in the top-up mode can be listed as follows:

(1) Larger vertical emittance of injection beam compared with the booster injector system,
(2) Larger energy jitter and spread of injection beam compared with the booster injector system,
(3) 2–3 macro bunches injection due to full energy injection with DC gun system,
(4) Vertical dispersion leakage due to different level between storage ring and linear accelerator, and
(5) Careful control of injected beam trajectory in vertical plane for reducing beam loss around a number of narrow gap in-vacuum undulators.

In order to resolve these problems, the following tasks were carried out. Two vertical slit systems were implemented to alleviate vertical emittance and the jitter of trajectory. Energy stability was also improved. One horizontal slit was installed in the dispersive region to alleviate energy jitter and spread. Energy acceptance of the ring was increased to capture two or three macro-bunches from linear accelerator. An additional corrector was installed to control injecting beam before the septum magnet. These improvements enabled the top-up injection in PLS-II. In this paper, we describe the overall top-up studies performed in PLS-II. In Sec. II, the PLS-II linear accelerator and the storage ring are introduced and Sec. III gives a theoretical description of beam motion during injection transient. Section IV shows the performance and experimental results of the top-up operation in PLS-II. Section V presents the

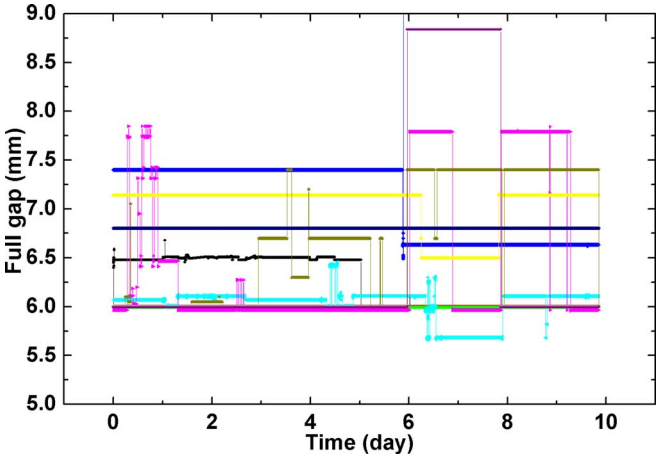

FIG. 1. Total 10 in-vacuum undulator gap motion for 10 days. Usually minimum full in-vacuum undulator gap is 6 mm.

future plan for increasing the performance of top-up operation. Finally, Sec. VI gives a summary and concluding remark.

II. DESCRIPTION OF PLS-II

Through the first year PLS-II operation, PLS-II performance was improved for satisfactory top-up operation. This section describes the machine characteristics and their improvement for the PLS-II top-up operation.

A. 3 GeV linear accelerator

PLS-II linear accelerator[3] consists of thermionic DC gun, S-band linear accelerator, and 86 m beam transport line. Forty six accelerating sections are installed along 164 m. The electron gun is the triode type with a < 1 ns or 250 ps grid pulser that generates short pulse. The bunching system (prebuncher and buncher) is located after the gun. Sixteen pulse modulators (200 MW and 7.5 μs for each modulator) and 16 klystrons (80 MW and 4 μs for each klystron) feed energy to beam up to 3 GeV. There are two beam analyzing stations at 100 MeV and 3 GeV, respectively. The beam transport line consists of three isochromatic systems, quadrupole magnets, and steer magnet that guide 3 GeV beam into the injection system of the storage ring. Table I lists the major parameters

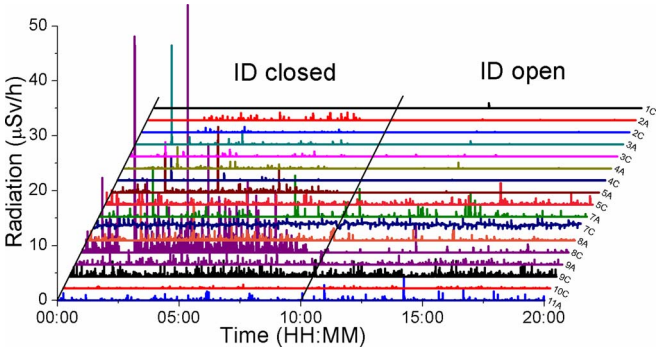

FIG. 2. Radiation doses in the beam line for all in-vacuum undulators (closed or open) during the top-up test.

TABLE I. Major parameters of the PLS-II linear accelerator.

Parameter	Unit	Value
Beam energy	GeV	3
Repetition rate	Hz	10
Energy stability	%	<0.2 rms
Energy spread	%	<0.3 rms
Emittance (normalized, rms)	μm rad	120
Gun pulse length (FWHM)	ns	1 or 0.25
SLED gain		1.5

of the PLS-II linear accelerator. The operation status of the klystron system is shown in Fig. 3, and this system is used in operating the 3 GeV linear accelerator with 97% availability. In order to diagnose beam energy and spread, the optical transition radiation (OTR) monitoring system was implemented after the first bending magnet in the beam transport system. The OTR target with 580 nm Al coated on 25 μm polyimide film gives minimum effect on beam characteristics. As a result, a non-destructive measurement of the beam energy is being applied during the top-up operation. Figure 4 shows the performance of the 3 GeV linear accelerator. Here one day performance is statistically treated for each data. Therefore, the total energy stability that includes short term effect by modulator and long term effect by temperature drift is kept at around rms 0.15%. During the first year PLS-II operation, the short term energy stability is improved to 0.05% rms due to De-Qing[4] application, and the long term temperature drift is corrected by the energy feedback system. In order to measure the beam energy with high resolution in the energy feedback system, Libera BPM[5] is used for trajectory reading with 10 Hz. In addition to the improvement of energy stability, the energy spread is controlled to below 0.25% rms.

At the beam analyzing station, after the 100 MeV pre-injector of PLS-II linear accelerator, the normalized horizontal and vertical emittances were measured at approximately 120 μm rad. This value corresponds to 20 nm rad un-normalized emittance at 3 GeV beam energy, and it is

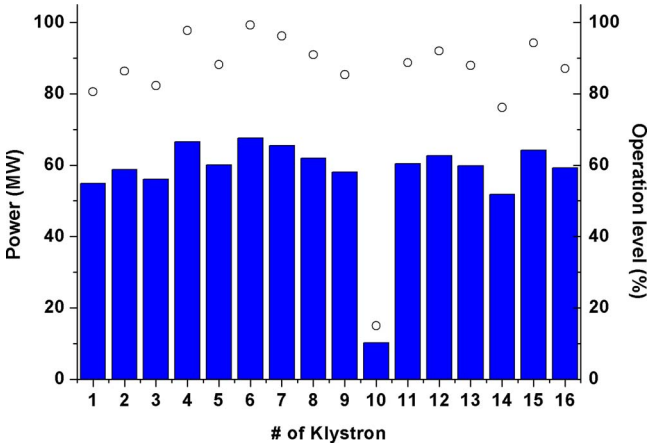

FIG. 3. Status of klystron operation. Bar indicates the operation power of the klystron. Circle indicates the percentage of operation level to maximum power level. Originally, the maximum power of the klystron was 80 MW with 4.0 μs pulse. Since the klystron is operating with 4.7 μs pulse, the maximum power is scaled down to 68 MW.

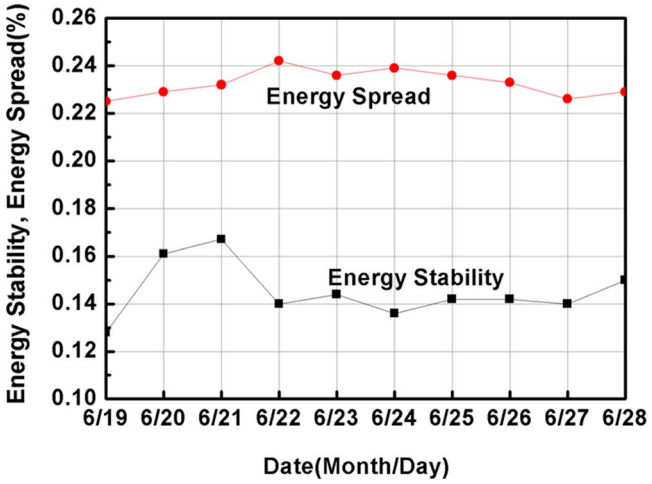

FIG. 4. Energy spread and stability measured by OTR system for 10 days.

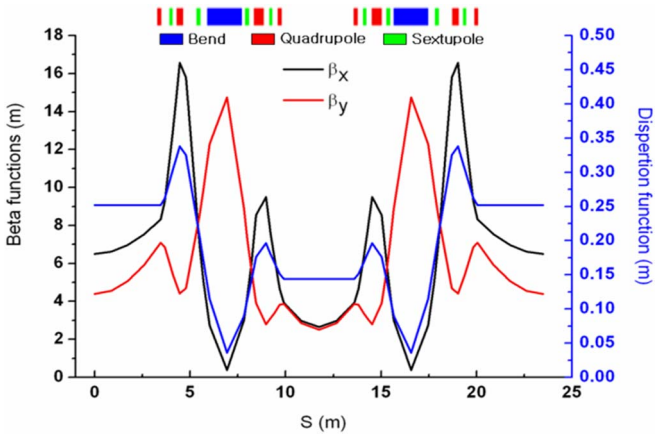

FIG. 6. Superperiod in a designed lattice for the 3.0 GeV ring and its optical functions.

comparable to the horizontal emittance of 5.8 nm in the storage ring. However, compared with the vertical stored beam emittance of 58 pm rad, the 20 nm rad vertical emittance of injected beam was too large to be used in the top-up operation. Note that the injected beam size at the narrow gap in-vacuum undulator ($<\pm 3$ mm full gap) is around 300 μm rms, and the edge of the beam can be lost if the vertical trajectory jitter of injected beam and the horizontal large oscillation are coupled toward vertical direction. Therefore, the need of a slit system is invoked in the beam transport system. Generally, a 90° separated two slit system in phase advance is useful in filtering the edge of the injected beam and in reducing the trajectory jitter effect. Figure 5 shows the vertical slit positions along the phase advance. In the figure, the schematic principle of emittacne reduction is also exhibited to describe the filtering of the injected beam edge. The phase advance along the linear accelerator and the beam transport line is calculated by ELEGANT[6] with initial lattice condition at the end of the pre-injector. To obtain the initial lattice condition at the end of the pre-injector, PARMELA code is used.

For careful control of injected beam, two Libera BPMs and one additional corrector were implemented. One additional corrector installed at the end of beam transport line is used to adjust the angle of the injected beam trajectory. Two Libera BPMs were installed at the beginning of the beam transport line (horizontal dispersive region) and at the end of beam transport line (vertical dispersive region), respectively. As a result, the shot to shot measurement stability of BPM system is improved by a factor of ten.

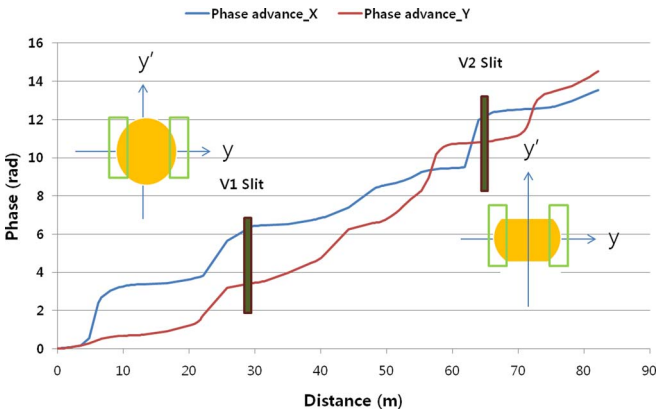

FIG. 5. Two vertical slit positions along the phase advance. Two vertical slit positions in the beam transport line of PLS-II are separated by a phase of around 80°. One horizontal slit as energy slit is located in the beginning of the beam transport line.

B. Storage ring

Figure 6 shows the lattice functions and Table II describes the main beam parameters for the PLS-II (The upgrade of Pohang Light Source). The lattice of the PLS-II has a gradient dipole double bend achromat structure with 12 superperiods. Each of the 12 superperiods contains two dipole magnets embedded in a FODO cell, a lattice period composed of a focusing (F) and a defocusing (D) quadrupole with a drift space (O) arrangement. The critical photon energy from bending magnets is 8.97 keV. The lattice provides one 6.88 m and one 3.69 m straight section per cell for installation of insertion devices. In order to reduce the beam emittance, a horizontal dispersion of 0.25 m is considered in the long straight section where RF cavities are installed. The 3 GeV linear accelerator in PLS-II is used as full energy injector to storage ring. The incoming electron beam from the beam transport line is horizontally parallel with the storage ring bumped orbit and is injected 8.234° vertically. The Lambertson magnet then bends the beam – 8.234° vertically to place it on the same level as

TABLE II. The main parameters of the PLS-II.

Parameter	Units	Value
Beam energy	GeV	3
Beam current	mA	400
Lattice structure		DBA
Superperiods		12
Emittance	nmrad	5.8
Tune		15.245/9.18
RF Frequency	MHz	499.97
Energy spread	%	0.1

TABLE III. Main design specifications of the PLS-II SC RF.

Parameter	Unit	Value
Harmonic Number		470
RF Frequency	MHz	499.66
Radiation Loss	keV	1242
Gap voltage	MV	3.3
Energy acceptance	%	2.6
Cooling capacity @4.5 K	W	700

the bumped orbit. For orbit bump, four kicker magnets are located within the 6.8 m free straight section in the storage ring.

The total scheduled user operation for the first year of 2012 was 3024 h with 93.8% reliability. Among the total of 13 user runs in 2012, the user runs up to 9th were serviced with normal RF cavities. From 10th run, the first super conducting RF module was used in the operation that significantly affected the reliability of PLS-II operation due mostly to the immature cryogenic system operation. However, through the winter shutdown between 2012 and 2013, the second SC RF module[7] was added in the operation resulting in larger energy acceptance in the storage ring. Table III lists the SC RF main parameters in 2013. Note that the NC RF system was operated with 1.8 MV gap voltage, and the SC RF system has been operated with 3.3 MV gap voltage. Here the energy acceptance increased from 1.4% to 2.6%, and the increased energy acceptance easily captured two macro bunches of injected beam during the injection.

In PLS-II, 30 beamlines are under user service, which include 14 insertion devices, 13 bending magnet beamlines, two diagnostics beamlines, and one independent fs-THz beamline. One wiggler, three out-vacuum undulators, and ten in-vacuum undulators are in operation. The typical gap of the in-vacuum undulator is 6 mm at present. In order to stabilize the orbit, a slow orbit feedback system is being run during user service. The feedback system uses the SVD (singular value decomposition) method and MATLAB channel access to EPICS IOC of BPMs and correctors. A total of 96 BPMs and 96 correctors for each plane are included in the slow orbit feedback system. Figure 7 shows the orbit stability for one service period which is 10 days. The Rms orbit variations for 10 days are 0.9 μm and 0.6 μm for horizontal and vertical plane, respectively. However, the orbit spike due to insertion device gap moving invokes the need for implementing the ID feed-forward.

III. INJECTION TRANSIENT

A. Injected beam motion

The septum location, orbit bump, and their shapes are designed considering the fact that the injected and stored bunches should not hit the septum magnet or any other part of the vacuum chamber during injection. Since the kickers K_1, K_2 and K_3, K_4 are symmetrically located on both sides near the center of the straight section and no optical elements are placed between kickers so that a bump orbit can be formed, the deflection angle of each kicker can be simplified as[8]

$$\Delta x_1' = -\Delta x_2' = -\Delta x_3' = \Delta x_4' = \frac{H_0}{L_{12}}, \tag{1}$$

where H_0 is the height of the orbit bump and L_{12} is the distance from the first kicker's center to the second one's center. Therefore, all kickers have the same magnitude of deflection angle. Furthermore, the orbit shape will remain the same despite the changes in the lattice parameters. Here, H_0 is 15 mm and L_{12} is 1590 mm. During the first three turns, the kicker strength follows:

$$\theta(n) = \theta_0 \cos(nT_r\pi / T_k), \tag{2}$$

where θ_0 is maximum integrated strength (9 mrad for PLS-II), n is the number of turns of the stored particles in the ring (n = 0 at injection), T_r is the revolution period of the ring, and T_k is pulse length of kicker field (6 μs for PLS-II). After three turns (i.e., the kicker is turned off), the betatron motion for central particle at the septum position is given by

$$x_c = A_{\max} \cos(2n\pi \upsilon_x + \varphi_0), \tag{3}$$

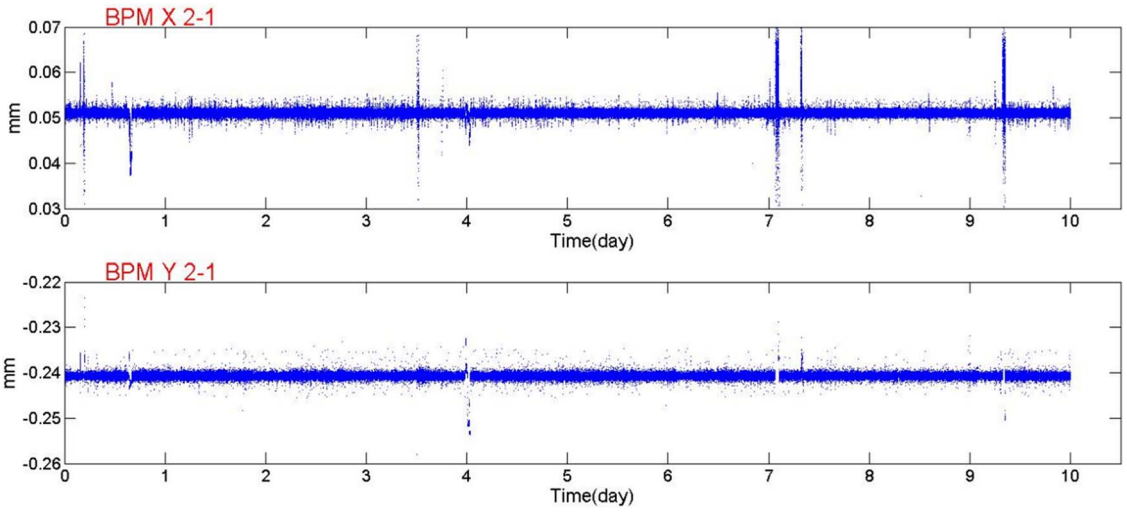

FIG. 7. Ten days orbit variation at the long straight section. The beta-functions are 6.5 m and 4.4 m for horizontal and vertical plane, respectively.

TABLE IV. Injected beam parameter.

Parameter	Unit	Value
Horizontal emittance	nm rad	20
Vertical emittance	nm rad	20
Energy spread	%	0.2
Bunch length	ps	100

where $A_{\max} = X_{injection} - H_0$, $X_{injection}$ is the horizontal coordinate for the injected beam at the septum position (29 mm for PLS-II), v_x is the horizontal tune, and φ_0 is the initial phase after three turns. During the first three turns, the betatron motion for central particle at the septum position is given by

$$x_c = H_0 \cos(nT_r\pi/T_k) + A_{\max}\cos(2n\pi v_x). \quad (4)$$

From Eq. (4), the horizontal positions of the bunch center during the first three turns with injection position (i.e., n = 0, 1, 2, 3) are −29 mm, −10.6 mm, 4.7 mm, and −8.9 mm, respectively.

We studied the transverse and longitudinal injection dynamics in detail by using ELEGANT. In the tracking, we launched 1000 particles distributed along the injected beam parameters. In the injected beam parameters from the PLS-II linear accelerator, the energy spread of injected beam is the factor two of the natural energy spread (i.e., energy spread of stored beam), and the bunch length of injected beam is set at rms 100 ps to represent the macro-bunches. Although 100 ps is larger than the actual bunch length, it is good enough to describe the statistical behavior of the macro-bunches with various timing differences between the linac and the ring. The other injected beam parameters used in the tracking are introduced in Table IV

Figure 8 shows the result of tracking studies on nonlinear effect for two cases of corrected chromaticity 0 and 5. Compared with the calculation of linear effect from Eq. (4), the septum clearance was reduced in the presence of sextupoles, since sextupoles produce amplitude-dependent tune shifts and thus change the betatron tune. However, this nonlinearity was found to be acceptable through tracking studies. The phase space distribution of the 1000 particles widened due to nonlinear effects and particle excursions along non-symmetry trajectory which resemble a 3rd order resonance pattern. Figure 9 shows the beam trajectory on the horizontal plane at the first turn. The position in the location of quadrupole family Q2 is about −20 mm; this is the largest position except in the injection region. The physical aperture in Q2 is 33 mm in horizontal plane. Therefore, it is enough to accommodate a −20 mm orbit deviation.

Figure 10 shows particle distribution in the vertical phase space at the exit of the PLS-II injection septum for ideal optics and trajectory control from beam transport line. The density contour plot represents the distribution of electrons for the incoming injected beam. Black and blue lines indicate dynamic acceptance and physical acceptance for in-vacuum undulator, respectively. The figure implies beam loss can be produced due to possible trajectory and coupling errors of injected beam.

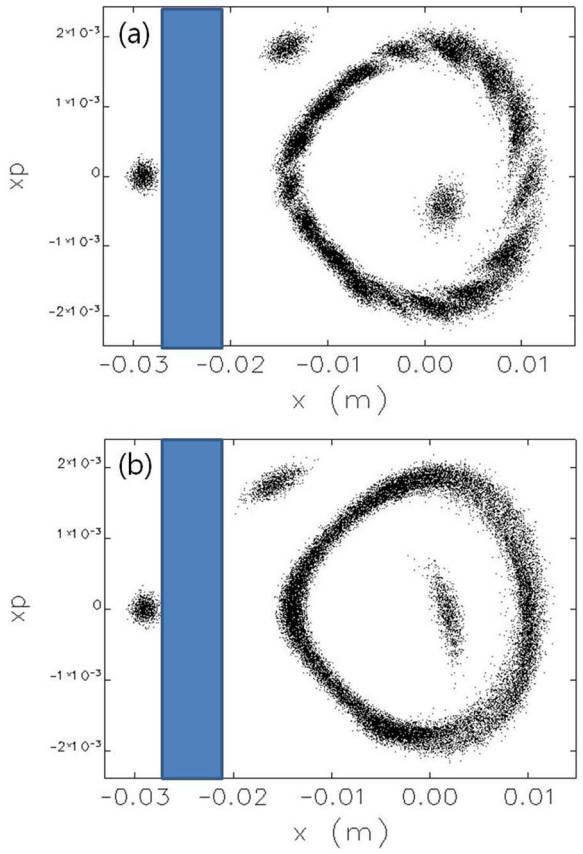

FIG. 8. Injected beam excursion with nonlinear effect in horizontal phase space during the first thirty turns for (a) corrected chromaticity 0 and (b) corrected chromaticity 5.

B. Stored beam perturbation

If the injection system has machine imperfection (i.e., tilt of bump magnets, non-similarity of magnetic field of bump magnets, the timing, amplitude and waveform errors for pulsed kicker magnets, leakage field from septum magnet, etc.), the stored beam will oscillate while the injection system is on; this oscillation seriously perturbs beamline experiments. Although a gating signal will be provided to beamlines

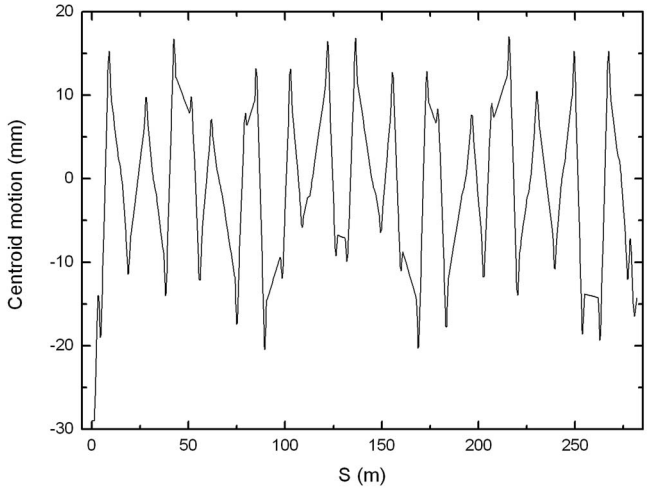

FIG. 9. Simulated horizontal beam trajectory at the first turn.

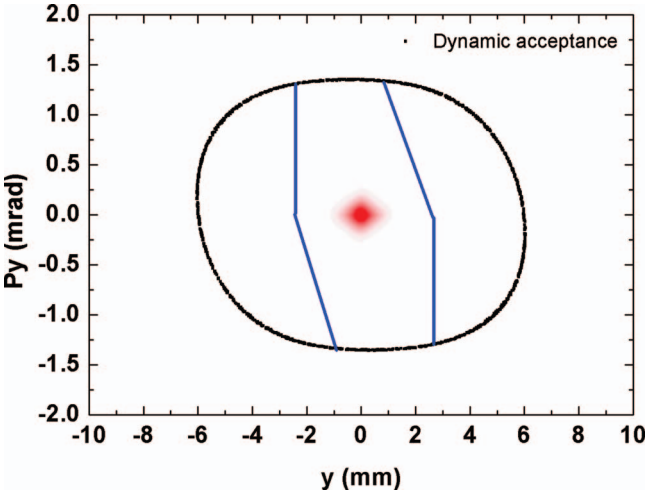

FIG. 10. Simulated injection beam distribution and acceptance in vertical plane. Red color exhibits high density and whitish color represents the edge of injected beam. Black and blue lines: dynamic acceptance and physical acceptance for in-vacuum undulator, respectively.

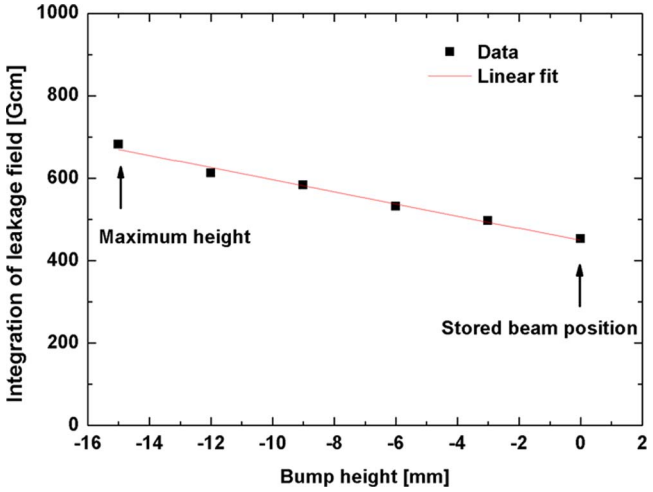

FIG. 11. The integration of leakage field versus bump height.

to enable masking of injection disturbance, the oscillation of stored beam should be kept tolerably small. Therefore, the estimation of stored beam perturbation due to the imperfection of injection system is important.

The main sources of stored beam perturbation in horizontal plane are the timing, amplitude and waveform errors for pulsed kicker magnets. In PLS-II, one kicker magnet power supply feeds power to K1 and K3 pair and K2 and K4 pair. Therefore, kicker timing can be adjusted between two pairs (i.e., K1 and K3 pair and K2 and K4 pair) in nanosecond scale. With consideration of flight time and the difference of cable length, the timing error between K1 and K3 (or K2 and K4) is less than a few nanoseconds. Compared with 6 μs pulse duration of kicker field, the effect of timing error can be negligible. Amplitude error of kicker field is also simulated, and the relation between residual horizontal oscillation and field error is evaluated as rms residual oscillation [μm] $\sim$ 34 $\times$ field error [%]. Waveform error of pulsed kicker field is the most serious source of the stored beam perturbation. However, estimation of the effect of waveform error is not easy due to the difficulty in measuring the pulsed kicker field.

The main sources of the stored beam perturbation in vertical plane are the leakage field from Lambertson septum magnet and the tilt of kicker magnets. The vertical orbit oscillation of the stored beam due to tile of bump magnets was estimated by ELEGANT. The relation between residual oscillation and tilt of bump magnets is obtained as rms residual oscillation [μm] $\sim$ 0.06 $\times$ rms tilt of bump magnets [μrad]. The stored beam is kicked by the leakage field, which depends on the orbit bump when the kicker field is applied on the stored beam during injection, as shown in Fig. 11. As a result, the stored beam is perturbed by vertical kick. The perturbation on stored beam can be described by

$$\begin{pmatrix} y \\ y' \end{pmatrix}_n = \begin{pmatrix} M_{33} & M_{34} \\ M_{43} & M_{44} \end{pmatrix}_{\text{One turn}} \begin{pmatrix} y \\ y' + \theta \end{pmatrix}_{n-1}, \quad (5)$$

where n is the index for turn number, θ is representing the kick induced by the leakage field in the septum magnet, and M is one turn transfer matrix. The kick by the leakage field along the kicker time profile and bunch is given by

$$\theta\,(n, L)\,[\mu\text{rad}] = 1.47 H_0 \sin\left(\frac{(nT_r + 2ns \times (L-1))}{T_k}\pi\right). \quad (6)$$

Here 1.47 is the linear fitting coefficient in Fig. 11, and H_0 is the maximum bump height, L is the bunch index (from 1 to 470), and T_r is the revolution period, T_k is the pulse length of the kicker field. By using one turn transfer matrix M of PLS-II lattice, the stored beam oscillation is calculated from Eq. (5), and the maximum amplitude of stored beam oscillation at the center of the long straight section is estimated as 100 μm. In PLS-II, both sources (the septum and the tilt of the kickers) are expected to have similar effect on the vertical perturbation on the stored beam. Although the source by the tilt of the kickers can be suppressed by careful alignment of the kickers, the source by the septum should be compensated rather than suppressed.

IV. TOP-UP OPERATION

In order to carry out the top-up operation in PLS-II, the radiation level (illustrated in Fig. 2) was improved by reducing the beam loss during injection. The main factors related with beam loss during injection are the narrow vertical physical aperture at the in-vacuum undulator and small horizontal clearance at the septum magnet. The vertical trajectory error and the large beam size of injected beam produce beam loss at the narrow gap aperture. Energy and horizontal trajectory errors produce beam loss at the septum position with operating tune. Considering these error sources, the sequence of the top-up injection was performed in the following order: (1) Phase and energy adjustment of injected beam. (2) Offset and angle tuning of horizontal injected beam. (3) Offset and angle tuning of vertical injected beam. (4) Reduction of slit gap in beam transport line. Figure 12 shows an image of streak camera when the injected bunches are captured in the RF bucket. It looks like two pairs of bunches, but it is actually a mirror symmetric image of a pair of bunches because of the setup of the streak camera. The bunches are separated by 350 ps,

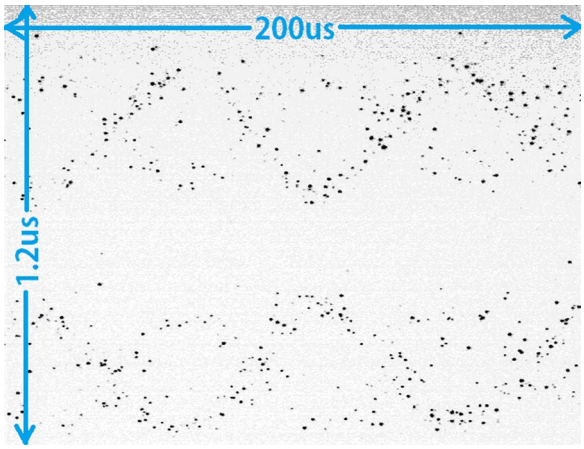

FIG. 12. Longitudinal injected beam measured by streak camera.

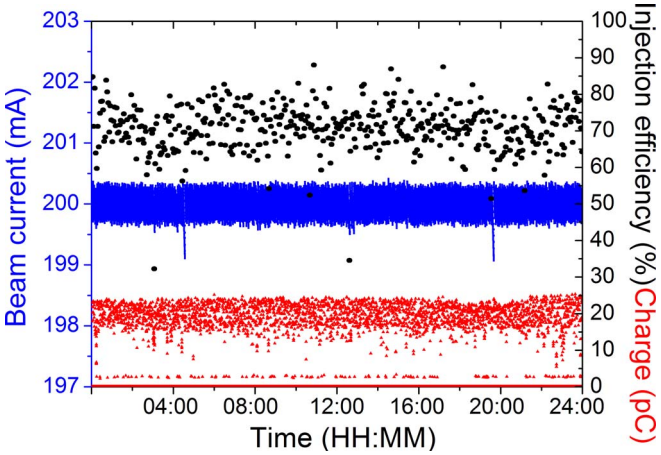

FIG. 14. Typical current regulation (blue), injection efficiency (black circle), and injected beam charge (red) during one day top-up operation after injection improvements.

which is a linac period, and they are oscillating with 10 kHz synchrotron frequency. The figure implies that the phase and energy of injected beam is satisfactory in the boundary of energy acceptance given by SR gap voltage. The open widths of the first slit and the second slit in the beam transport line are 1.6 mm and 1.1 mm, respectively. The radiation dose in the beam line after following the setup procedure of top-up injection is shown in Fig. 13. Compared with the result of the top-up injection in 2012, the radiation doses are improved by a factor of 40. Excepting around 1 μSv/h in 3A beam line, radiation dose is background level of detector.

After improving the radiation dose in the beam line, the top-up injection has been in operation in PLS-II since March 2013. The typical current regulation, injection efficiency, and injected beam charge during one day top-up operation are shown in Fig. 14. The beam current is regulated with rms 0.09% at 200 mA, the average injection efficiency is 70%, and the charge of injected beam is kept blow 25 pC. When the transport line slits are open, the charge of injected beam is 100 pC, and the injection efficiency is 35%. The 10 Hz shot by shot measurement of injection efficiency and injected beam charge was enabled by the sum data from Libera BPM implemented at the end of the beam transport line. During the 8 h of top-up mode operation, the photon flux was also measured at the supramolecular crystallography beam line. The experimental equipment in the beam line is adjusted at 17.7 keV and the flux is measured by the ion chamber just 30 cm from the sample position. Photon flux change (ΔI) is 2% for 8 h, 0.5% at every 3 min of injection, and 0.4% during the 3 min between injections. Compared with the 40% flux reduction during the decay mode operation, the flux changes during the top-up operation are remarkably improved. However, the 0.5% systematic flux dip every 3 min is due to the stored beam perturbation by the imperfection of the injection system as illustrated in Fig. 15.

V. THE FUTURE PLAN

Due to 300 μm stored beam oscillations in both planes during injection, the flux dips of the 30 beam lines at PLS-II range from 1% to 8% during injection. Therefore, the 300 μm stored beam oscillations by the imperfect injection system should be suppressed to improve photon flux changes in the top-up operation. Especially, the vertical oscillation should

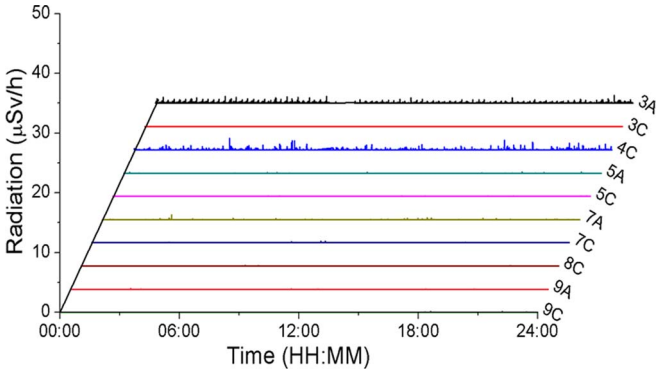

FIG. 13. Reduction of radiation dose in the beamline for all in-vacuum undulator with minimum gap during top-up injection compared with Fig. 2, the radiation dose after injection improvements disappeared almost.

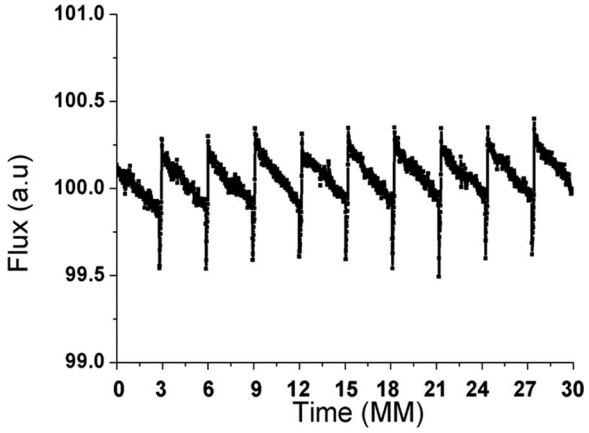

FIG. 15. Photon flux at supermolecular crystallography beam line 30 min after injection improvements. For 8 h, the flux change becomes larger due to the effect related with the photon beam stability, but it is only 2% in the top-up mode operation.

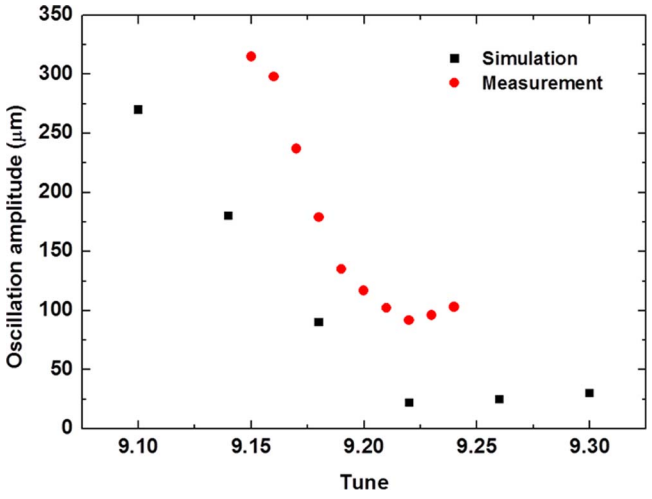

FIG. 16. Vertical stored beam oscillation along vertical tune. There is a clear improvement at 9.22, but for some beam dynamic issues, the operations are still at 9.15.

be drastically suppressed since the beam sizes in the long insertion device straight section are approximately 320 μm and 20 μm for the horizontal and vertical plane, respectively (190 μm and 10 μm in the short insertion device straight section and 60 μm and 30 μm in the bending magnet). In order to suppress the vertical stored beam oscillation during injection, tune adjustment and leakage field compensation are recommended.

Adjustment of vertical operation tune can reduce vertical oscillation by leakage field from the septum magnet. In Eq. (5), each transfer matrix element can be manipulated by adjusting vertical tune, and the effect of the leakage field kicks along the height of the bump orbit can be increased or decreased depending on the transfer matrix element. Figure 16 shows the result of the tune adjustment by simulation as well as the measurement. In the figure, the vertical oscillation amplitude by the septum leakage field can be suppressed to less than 20 μm at the vertical tune of 9.22 in the simulation. In the real measurement, 100 um stored beam oscillations as minimum value still remain at the vertical tune of 9.22. The discrepancy might be caused by the kicker tilt error, which was not accounted for. However, a detailed beam dynamics study is necessary to confirm the reliability of operation at this tune.

Leakage field compensation minimizes θ in the right hand side of Eq. (5). In general, the field compensation magnet around the septum magnet is employed to suppress the stored beam oscillation by leakage field as in the implementation of the skew bending and quadrupole magnets at both end sides of the septum magnet. However, the use of skew bends and skew quadrupole introduces additional coupling problems, and, in principle, the space in the injection region should be available for these magnets. Recently, Taiwan Photon Source and SPring-8 have used the remote control for tilting the kicker magnet to reduce its vertical field effect. The function of tilt control works quite well in suppressing vertical oscillation up to a 5 μm oscillation amplitude in SPring-8. By tilting the kicker magnet deliberately as shown in

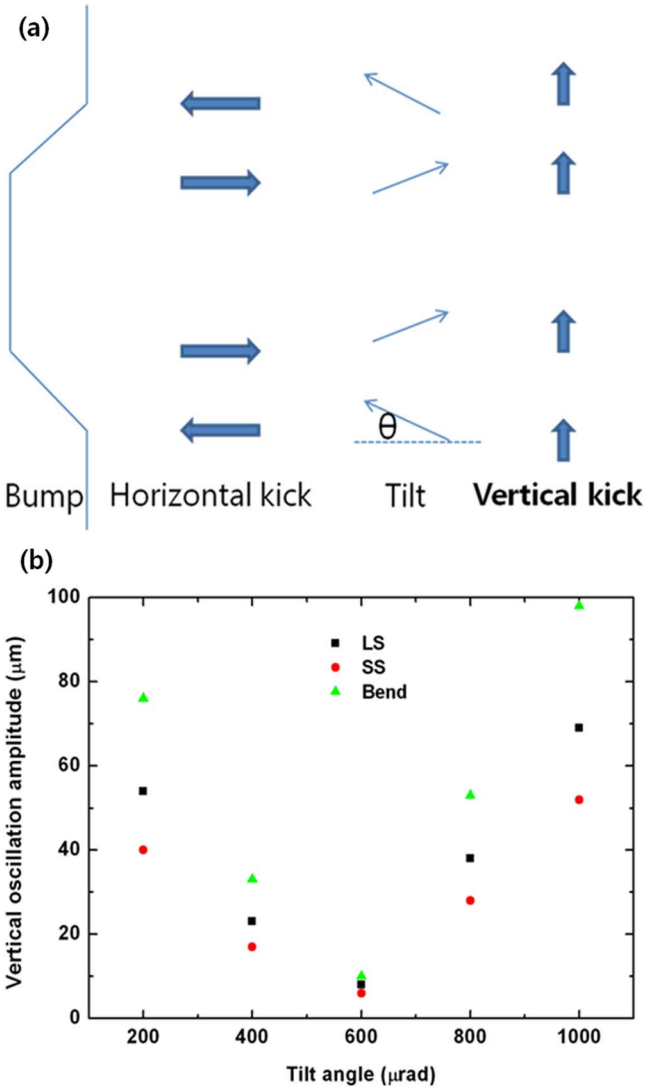

FIG. 17. (a) Schematics for generating vertical kick from kicker magnet for compensating linear leakage field from septum magnet. (b) Vertical stored beam oscillation along kicker magnet systematic tilt.

Fig. 17(a), the vertical kick from the kicker magnet can be used for compensating the linear septum leakage field as in Fig. 11. This method is preferred to compensate the leakage field of the septum magnet since the remote control for tilting the kicker magnet will be installed to correct the kicker tilt error as well. Figure 17(b) shows the simulation result of the kicker tilt effect. As shown in the figure, the stored beam oscillation is suppressed below 10 μm in the case of 600 μrad tilt.

Through the simulation study, suppressing the stored beam oscillations during injection up to beam size level is expected to be achievable soon. However, a new injection system should be studied and planned to suppress the stored beam oscillations to less than the beam size. To solve the difficulty of handling unbalanced waveforms between kickers due to their strong and short pulse in the present series kicker connection, feasibility studies for individual kicker power supplies and pulsed sextupole magnet injection[9] have been conducted in PLS-II.

VI. SUMMARY

After overcoming the unfavorable situations for top-up injection, PLS-II has been operating top-up injection since 19th March 2013. The unfavorable situations were larger vertical emittance and energy jitter due to full energy injection by the linear accelerator, at least ten narrow gap in-vacuum undulators with 6 mm full gap, and different levels between the linear accelerator and the storage ring in PLS-II. To overcome these unfavorable situations, we made the following adjustments: (1) Energy acceptance is increased from 1.4% to 2.6% by running two superconducting cavities. (2) Energy stability is improved in the linear accelerator by applying De-Qing and Libera BPM in the energy feedback system. (3) Beam loss in the narrow gap in-vacuum undulator in the storage ring is reduced by filtering the edge of the injected beam in phase space. As a result, top-up operation has been provided for user service, the beam current has been regulated with rms 0.09% at 200 mA, and the flux change for 8 h is improved from 40% in decay mode to 2% in top-up operation at the supramolecular crystallography beam line. In order to improve the stored beam oscillation that is less than the beam size during injection, studies are under way for two possible upgrades of the PLS-II injection system (individual kicker power supplies and pulsed sextupole magnet injection), in addition to the tune adjustment and compensation of the linear septum leakage field.

ACKNOWLEDGMENTS

We thank Professor Helmut Wiedemann (SLAC), M. Boege (SLS), and M. Takao (SPring-8) for their graceful comments. This research was supported by the Converging Research Center Program through the Ministry of Science, ICT and Future Planning (Grant No. 2013K000306).

[1]H. Ohkuma, *Top-up Operation in Light Sources*, EPAC08, Genoa, Italy, June 2008, MOZCG01.
[2]S. Shin, Commissioning of the PLS-II, JINST, January 2013.
[3]B.-J. Lee, PLS-II Linac upgrade, IPAC2012, New Orleans, USA, May 2012, WEPPD069.
[4]S. H. Kim, Development and management of the modulator system for PLS-II 3.0 GeV electron linac, IPAC2012, New Orleans, USA, May 2012, THPPD073.
[5]See http://www.i-tech.si/accelerators-instrumentation/libera-brilliance-plus/benefits_1 for high resolution Libera BPM.
[6]M. Borland, Elegant: A flexible sdds-compliant code for accelerator simulation, No. LS-287, 2000.
[7]M.-H. Chun, Operation status of RF system for the PLS-II storage ring, IPAC2013, Sanghai, China, May 2013, MOPEA048.
[8]K. Fan, Nucl. Instrum. Methods Phys. Res., Sect. A **450**, 573–578 (2000).
[9]H. Takaki, Phys. Rev. ST Accel. Beams **13**, 020705 (2010).